





# SUstainable solutions for affordable REtroFIT of domestic buildings

Call: H2020-LC-SC3-2018-2019-2020

Topic: LC-SC3-EE-1-2018-2019-2020

Type of action: IA

Grant Agreement number	894511	
Project acronym	SUREFIT	
Project full title	<b>SU</b> stainable solutions for affordable <b>RE</b> tro <b>FIT</b> of domestic buildings	
Due date of deliverable	30/11/2021	
Lead beneficiary	University of Nottingham (UNOTT)	
Other authors	Instituto de Soldadura e Qualidade (ISQ)	

WP4 - Deliverable D 4.5 Evaporative cooling unit



#### **Dissemination Level**

PU	Public	X
со	Confidential, only for members of the consortium (including the Commission Services)	
Cl	Classified, as referred to in Commission Decision 2001/844/EC	

#### **Document History**

Version	Date	Authors	Description
1	30/11/2021	University of Nottingham	First draft of D4.5
2	12/01/2022	ISQ	Coordinator review
3	03/02/2022	ISQ, UNOTT, FSMR	Contribution from partners
4	27/04/2022	University of Nottingham	Final version

#### Disclaimer

This document is the property of the **SUREFIT** Consortium.

This document may not be copied, reproduced, or modified in the whole or in the part for any purpose without written permission from the **SUREFIT** Coordinator with acceptance of the Project Consortium.

This publication was completed with the support of the European Commission under the *Horizon 2020 research and innovation programme*. The contents of this publication do not necessarily reflect the Commission's own position. The documents reflect only the author's views and the Community is not liable for any use that may be made of the information contained therein.

This project has received funding from the European Union's Horizon 2020 research and innovation programme under grant agreement No **894511**.



# Contents

1	Summary	9
2	Introduction	11
	2.1 Hollow fibre integrated evaporative cooling system	11
	2.2 Permeable polymer hollow fiber dehumidifiers	12
	2.3 Desiccant material	12
	2.4 System description	13
3	Design and development of evaporative cooling unit	18
	3.1 Liquid desiccant dehumidification and cooling system	18
	3.2 Building and climate description	18
4.	System performances	20
	4.1 Effect of the inlet air conditions	20
	4.2 Effect of the liquid desiccant solution inlet conditions	24
	4.3 Effects of the dimensionless parameters	26
C	Conclusions	30
R	References	31





# Table of figures

Fig. 1. Cooling units: PEC indirect cooler (left), PEC core (middle) and fibre cooler (right)	9
Fig. 2. Schematic diagram of polymer hollow fibre integrated liquid desiccant dehumidification system	14
Fig. 3. The 3-D model image of the hollow fibre dehumidifier module	15
Fig. 4.The polymer hollow fibre integrated liquid desiccant dehumidification testing rig (A) and the	
connections with the environmental chamber (B)	16
Fig. 5. Polymer hollow fibre liquid desiccant air dehumidification and cooling cycle	18
Fig. 6. Diagram of a domestic installation of Liquid desiccant dehumidification and cooling system	19
Fig. 7. The dimensionless parameters variations under different air velocities (Tair,i= 35°C, Tsol,i=29.5°C,	
msol, i=0.028kg/s, RH <sub>air,i</sub> =60%, X <sub>sol</sub> =62%)	21
Fig. 8.The numerical obtained outlet air temperature (A) and specific humidity difference (B) under various air	
velocities (T <sub>sol,i</sub> =29.5°C, msol, i=0.028kg/s, RH <sub>air,i</sub> =60%, X <sub>sol</sub> =62%)	22
Fig. 9. The numerical obtained sensible effectiveness (A) and latent effectiveness (B) under different inlet air	
velocities (T <sub>sol,i</sub> = 29.5°C, msol, i=0.028kg/s, RH <sub>air,i</sub> = 60%, X <sub>sol</sub> = 62%)	23
Fig. 10. Variations of sensible effectiveness (A) and latent effectiveness (B) for several inlet solution temperature	<u>'S</u>
at various solution concentrations ( $T_{air,i}$ = 35°C, $RH_{air,i}$ =60%, $V_{air,i}$ =3.6m/s, $msol, i$ =0.028kg/s)	. 25
Fig. 11. Variations of latent and sensible effectiveness with the solution mass flow rate ( $T_{air,i}$ = 35°C, $T_{sol,i}$ = 29.5°C,	
RH <sub>air,i</sub> = 60%, X <sub>sol</sub> = 62%, V <sub>air,i</sub> = 3.6m/s)	26
Fig. 12. Variation of the outlet air temperature and sensible effectiveness with the air to solution specific humidi	ty
ratio ( $T_{air,i}$ = 35°C, $T_{sol,i}$ = 29.5 °C, $msol$ , $i$ == 0.028 $kg/s$ , $V_{air,i}$ = 3.6 $m/s$ )	27
Fig. 13. Variation of the specific humidity difference and moisture removal rate with the air to solution specific	
humidity ratio ( $T_{air,i}$ =35°C, $T_{sol,i}$ =29.5 °C, $msol, i$ = 0.028 $kg/s, V_{air,i}$ =3.6 $m/s$ )	28
Fig. 14. Variation of the latent effectiveness and total effectiveness with the air to solution specific humidity ratio	0
$(T_{air,i}=35~^{\circ}\text{C}~,~T_{sol,i}=29.5~^{\circ}\text{C}~,~msol,i=0.028~kg/s,~V_{air,i}=3.6~m/s)$	28

27/04/2022

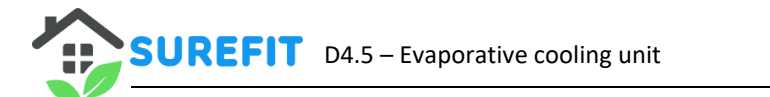




# **Table of tables**

Table 1 Ph	vsical pro	operties o	f the r	oolvmer hollow	fibre module1	6



# **Abbreviations**

COP Coefficient of performance

PEC Psychrometric energy core

PHFD Polymer hollow fiber dehumidifiers

PVDF Polyvinylidene fluoride

GWP Global Warming Potential

RH Relative Humidity

PVDF Polyvinylidene flouride



# **Publishable summary**

A polymer hollow fibre liquid desiccant unit is presented including experimental, numerical, and building performance analysis. A polymer hollow fibre liquid desiccant system for air dehumidification and cooling is proposed and analysed numerically. A numerical model for the core of the system is developed and validated with experimental measurements. The model is then coupled to a simplified model of a regenerative cycle of the liquid desiccant solution. Once the models are developed and validated, a parametric analysis for the core of the system and regenerative cycle is conducted aiming to access the performance for different working conditions.



#### Introduction

**Leading Beneficiary: University of Nottingham (UNOTT)** 

Participants: Instituto de Soldadura e Qualidade (ISQ)

#### Task description:

The work package involves fabricating and testing the key components and assembling the components into complete prototypes of technologies. The technologies will be tested in the lab to assess their performance under the nominal set conditions. The testing results will be used to modify and improve the design of the final prototypes, if necessary, which will be used in WP6 (field tests). The availability of this prototype system for field trials will be milestone 3. UNOTT is the work package leader.

Task 4.2: Produce solutions for energy efficient facilities (UNOTT, M7-M17)

• UNOTT will produce novel evaporative coolers.

This deliverable concerns the demonstrator planned for Deliverable 4.5- Evaporative cooling units.



# 1 Summary

Air-conditioning systems consume substantial amounts of energy with an accompanied peak demands on the electricity supply infrastructure contributing to a large proportion of carbon dioxide emissions. Evaporative cooling is a highly energy efficient alternative where applicable. Dew point cooling could decrease the air temperature close to the dew point without moisture increase, so it maximises the cooling capability of the dry air, but most of the dew point cooling heat exchanger is complicated and not easy to make and also costly and not suitable for large airflow. This document report the proposed innovative Psychrometric Energy Core (PEC). Figure 1 shows the basic structure of this novel dew point core for the proposed evaporative cooling system developed by UNOTT (UK Patent, Air conditioning, WO 2010/034994). This novel dew point core takes the same structure of the evaporative cooling pad structure. It has both advantages of the evaporative cooling pad, and dew point cooling, but without the drawbacks described above. Two core techniques are included in the novel cores, namely special corrugated plates for dew point cooling, and special sealing technology for the sealing. The core could be easily be enlarged to treat large airflow without increase in pressure drop. The initial development of a psychrometric energy core (PEC) prototype has already been carried out by partners.







Fig. 1. Cooling units: PEC indirect cooler (left), PEC core (middle) and fibre cooler (right)

The key innovations are summarized as follows:

- i. The proposed novel evaporative cooling system uses fibres that is cost effective and energy efficient.
- ii. The cooler utilises membrane fibre with 5000 hollow fibres. The developed evaporative cooler configuration allows cross-flow heat and mass exchange between hot air flow in the duct and water flow in the hollow fibres, attaining a high COP of about 12 when renewable heat and electricity are integrated.
- iii. Indirect evaporative cooling enables the ambient air to be cooled without increasing its moisture considerably.
- iv. The PEC is made of pad structures (e.g. polymer/wick) that absorb and hold moisture and gives maximum surface area for air and water contact. The wick is separated by thin plastic sheets and impregnated with unique ingredients and additives to achieve a high performance and structural strength. The PEC Pads are also treated with anti-rot chemical, which helps to prevent algae, bacteria or fungus.



v. The performance of such a system depends on the type and performance of the heat exchanger. To obtain a highly efficient indirect evaporative cooling system, a highly effective heat exchanger should be used. A newly developed air-cooling unit comprising a psychometric energy core (PEC) could decrease the air temperature close to the dew point without moisture increase, so it maximises the cooling capability of the dry air.

27/04/2022



#### 2 Introduction

#### 2.1 Hollow fibre integrated evaporative cooling system

Global energy demand is soaring during past few decades due to the rapid worldwide economy development and urban sprawl. According to the research report produced by International Institute of Refrigeration, air conditioning system accounts for 45% of the total energy consumption for domestic and commercial buildings [1]. Overall, air-conditioning system takes up approximately 15% of the total energy consumption around the world [1]. In the Middle East, where the climatic condition is hot and humid, air conditioning system consumes as high as 70% of energy required for buildings and around 30% of the total energy [2]. With the impact of global warming, the demands of effective air-conditioning system which consumes less energy and provides higher cooling performance is massive.

The current widely-used vapour compression system plays dominant role in the market. However, vapour compression system has the disadvantages of intensive energy consumption and low performance in hot and humid climate. Moreover, the possible leakage of high global warming potential (GWP) refrigerants will lead to the depletion of the ozone Layer, which will further contribute to the global warming and other associated environmental and social changes. Hence, the development of more energy efficient and environmentally benign cooling systems remains to be a highly researched topic.

Many attempts have been made by researchers with the aim to replace mechanical vapour compression system with other environmentally friendly air conditioning system with low carbon emission. With the advantages of a low grade energy use and environmentally benign refrigerants, as well as being simple in construction, air conditioning systems such as adsorption system, ejector cooling system and evaporative cooling system have been proposed and demonstrated in many niche applications [3-6]. Adsoprtion or absorption system [5] and ejector system [4] could be driven by low grade energy or industrial waste heat. However, these systems contain many components which sometimes cannot easily be manipulated. Besides, the performance of these systems is relatively low (Coefficient of performance (COP) around 0.2-0.5), which remains to be a major drawback for the wide application in the market. With water as the major working fluid and driven by the latent heat of evaporation, evaporative cooling system serves as another sustainable alternative for air conditioning technology. Recently, evaporative cooling system has been studied extensively by researchers, with focus on pad incorporated evaporative cooling system [7-10], desiccant based evaporative cooling system [11, 12], and dew point based evaporative cooling system [13-16]. Due to the large contact surface area, porous pad incorporated evaporative cooling systems have attracted more attentions. Wu et al. [17] presented a simplified mathematical model to describe the heat and moisture transfer between water and air in a direct evaporative cooler, with pad thickness of 125mm and 260mm, the cooling efficiency reached 58% and 90% respectively. Franco et al. [18] studied the influence of water and air flows on the performance of cellulose media. The results showed that with a thickness of 85mm, a plastic grid pad could offer a cooling efficiency of 65% at wind speed of 1.5m/s. However, since water is directly in contact with the incoming air in the closed system, there is the potential for microbial growth due to the supply of stagnant water. This will provide an opportunity for the spread of liquid phase-born bacterial diseases for occupants [19].



In order to solve this problem, the hollow fibre integrated evaporative cooling system [20] has been proposed. Compared with porous pad media, hollow fibre materials provide several advantages as following: 1) allow selective permeation of moisture: with pore sizes less than 0.1µm, hollow fibre material will allow the water vapour transfer but eliminate the bacteria and fungi penetration [21]; 2) provide large surface area per unit volume [22], which is favourable for enhanced heat and mass transfer. According to Chen et al. [23], the overall heat transfer coefficients could reach up to 1675W/m2K with a fibre diameter of 550µm. Kachhwaha and Preahhakar [24] analysed heat and mass transfer performance for a direct evaporative cooler using a thin plastic plate.

#### 2.2 Permeable polymer hollow fiber dehumidifiers

Despite their advantages, a main problem with the above systems is that droplets of the desiccant migrate across the dehumidifier, carried by the air passing over the liquid surface. Since most liquid desiccant materials (LiCl, CaCl2 and LiBr) are corrosive and harmful to health, the spreading – and the need of the subsequent removal – of their carryovers becomes a significant disadvantage.

In order to solve this liquid carryover problem, permeable polymer hollow fiber dehumidifiers (PHFD) have been proposed as an alternative for direct contact dehumidifiers [23, 24]. In PHFDs, the incoming air is circulated across a hollow fiber bundle, inside which the liquid desiccant is flowing through. Thanks to its small pore size (less than  $100\mu m$ ) [25], the porous wall of the hollow fibre allows the moisture of the incoming air to penetrate into the liquid desiccant flow inside the fibre, while preventing any liquid desiccant from spilling into the processed air.

#### 2.3 Desiccant material

As the key element in a desiccant cooling system, the desiccant is a material that has a significant capacity of holding water. The moisture transfer between the air and the desiccant is generally driven by the difference in vapour pressure. When the vapour pressure of the air is greater than that of the desiccant, the moisture will be transferred from the air to the desiccant, and vice versa. Desiccant materials used can be either solid [25, 26] (e.g., silica gel, molecular sieve) or liquid [25] (e.g., lithium chloride (LiCl), calcium chloride). Liquid desiccants have quite a number of merits compared with solid desiccants. The ability of liquid desiccant to hold moisture is normally greater than that of solid desiccants. Besides, the regeneration temperature of the liquid desiccant is mostly between 40°C and 70°C[27], which is much lower than that required by the solid desiccant (in the range of 60–115°C)[26]. This makes it possible for the liquid desiccant cooling system to be incorporated with low grade heat sources (solar energy or waste heat).

Lithium chloride (LiCl) solution is the most stable liquid desiccant, which offers the lowest water vapour pressure and dehydration concentration 30-40% [28]. Calcium chloride (CaCl2) solution is the cheapest and most widely available desiccant, but it has the disadvantages of being unstable, depending on the air inlet conditions and the solution concentration rate [29]. Lithium bromide (LiBr) solution offers similar characteristics during dehumidification and regeneration process, but the cost of LiBr is about 20% higher than LiCl [30]. The mass transfer performance of LiBr and CaCl2 solutions are compared theoretically by Lazzarin et al.[31]. The author concluded that based on the same temperature and crystal temperature, LiBr showed better heat and mass transfer performance than that of CaCl2 solution. A mathematical model for an



adiabatic counter flow dehumidifier was developed by Kornnaki et al.[32], with three different desiccant solutions (LiCl, CaCl2 and LiBr). At the inlet air temperature and humidity of 30-42 °C and 13.0 g/kg, the absorption efficiency was 0.145, 0.137 and 0.125 respectively for LiCl, LiBr and CaCl2. Longo and Gasparella[33] examined the energy saving effect of three different liquid desiccants (LiCl, KCOOH and LiBr) in a real flower greenhouse application during three years' time span. The greenhouse equipped with such desiccant based air conditioning system exhibited the energy saving of 9.6%, 11.7% and 15.1% respectively for using the desiccants of LiCl, KCOOH and LiBr. The above-mentioned three salts (LiCl, CaCl2 and LiBr) have the disadvantages of corrosive feature, which can cause significant damage to air conditioning system. As a less corrosive and more environmentally friendly solution, potassium formate (KCOOH) solution has recently been applied in desiccant cooling unit. KCOOH solution has the advantages of less corrosive, less expensive to manufacture, and of low toxicity and viscosity compared with LiBr, LiCl and CaCl2[34]. Apart from such environmentally friendly features, KCOOH has higher vapour pressure, which potentially require less energy input during the regeneration process [34]. However, to date, the cooling and dehumidification performance of KCOOH was hardly revealed in the literature.

#### 2.4 System description

A testing rig was manufactured and developed at the laboratory of University of Nottingham to experimentally investigate the dehumidification performance of proposed novel polymer hollow fibre integrated liquid desiccant cooling system under various testing conditions. The testing rig comprises a polymer hollow fibre dehumidifier, an air tunnel, a circulation pump, a fan, a water filter and a two solution tank. The detailed schematic diagram is shown in Figure 2. The aluminium air tunnel was connected with a variable frequency drive centrifugal fan, which was linked directly with the environmental chamber. The environmental chamber could provide hot and humid air with temperature in the range of 10-50 °C, and relative humidity (RH) in the range of 0-75%. Two 8-litre plastic tanks were used as the strong solution and weak solution reservoir to store the liquid potassium format solution. In order to avoid any particle blockage within the polymer hollow fibres, a water filter was allocated before the entrance of the hollow fibre dehumidifier to improve the purity of the incoming liquid desiccant into the fibres. A flow meter and a ball valve were placed before the entrance of the liquid desiccant solution into the hollow fibre dehumidifier to control the solution flow rate inside the fibre.

Strong desiccant solution was pumped by a 25 W single phase centrifugal pump, from the solution tank to the top of the hollow fibre dehumidifier. In order to ensure the uniform distribution of the liquid desiccant solution into the hollow fibre module, a rectangular shape copper frame with 1mm holes on the sides of the frame was placed on top of the hollow fibre dehumidifier. Liquid desiccant was sprayed from the holes of the copper frame and flew down the hollow fibre dehumidifier by gravity. After getting contact with the incoming air, the weak solution was directed into another weak solution tank via a T-piece tubing. The weak solution was then pumped into the regenerator, which was made from an aluminium plate heat exchanger. The regenerator was connected with a 3kW electrical boiler. This boiler could provide hot water up to 80°C, with the purpose to regenerate the liquid desiccant. After the regeneration,



the concentration of the diluted solution was increased to a higher level. It was finally pumped back by the pump to the strong solution tank to complete the cycle.

The polymer hollow fibre module consists of 5000 fibres, which were sealed at each end to a plastic plate using adhesive sealant. The entire polymer hollow fibre module is contained in a plastic box. The height of the polymer hollow fibre dehumidifier is 0.5m, while the cross section diameter of the module is 0.2m. Polyvinylidene fluoride (PVDF) hollow fibres with outside diameter of 1.6mm and inside diameter of 1.4mm, an effective pore size of 0.5µm and a porosity of 50% were used for the fabrication of the polymer hollow fibre dehumidifier. It is important to note that, the utilization of the porous hollow fibre not only allows the penetration of the water vapour from the incoming air into the liquid desiccant solution, but also helps to prevent liquid desiccant droplets migrating across the dehumidifier. Thus, the conventional problems of solution carryover in liquid desiccant cooling system could be avoided. The detailed 3-D model and the actual testing prototype image of the hollow fibre module is shown in Figure 3 and Figure 4, respectively. The detailed geometrical, physical properties of the polymer hollow fibre module and the experimental working conditions were summarized in Table 1.

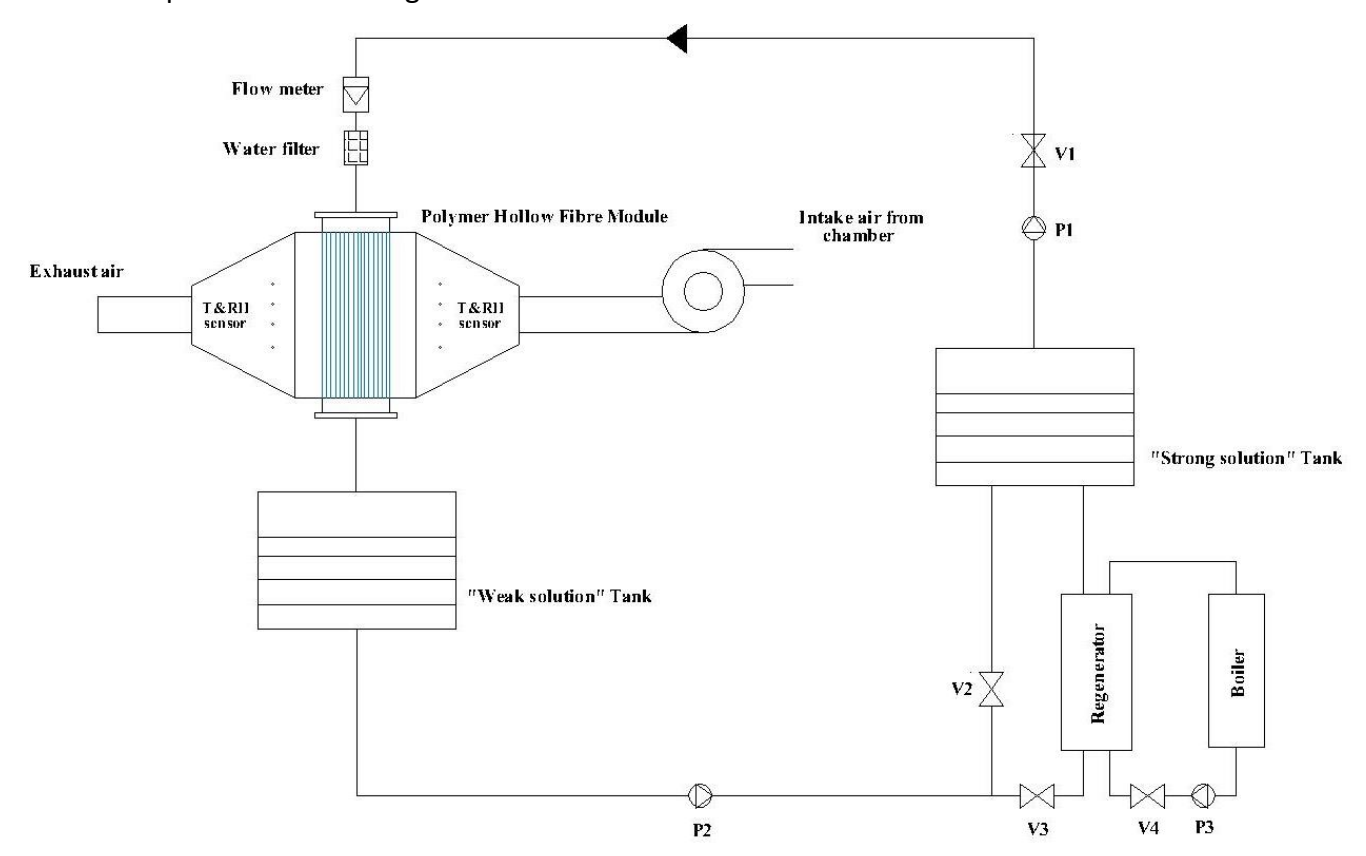


Fig. 2. Schematic diagram of polymer hollow fibre integrated liquid desiccant dehumidification system





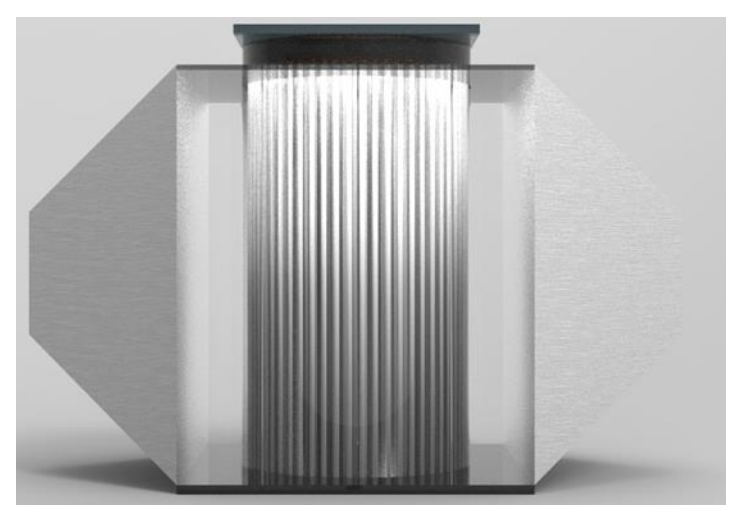


Fig. 3. The 3-D model image of the hollow fibre dehumidifier module

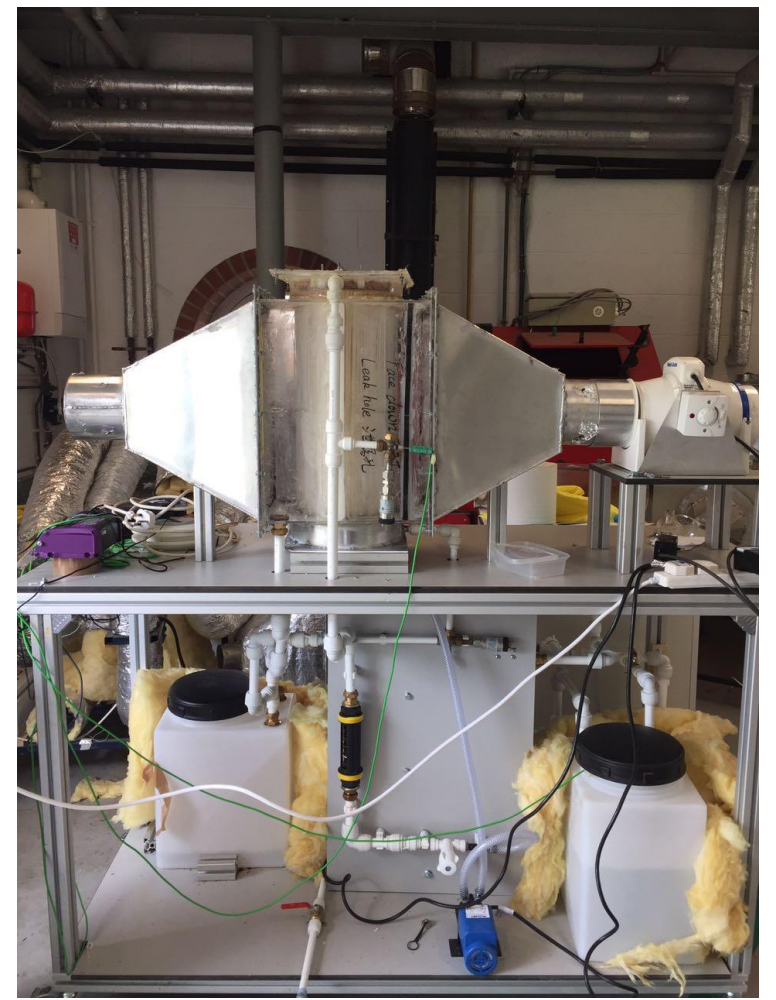


Figure 4(A) The polymer hollow fibre integrated liquid desiccant dehumidification testing rig





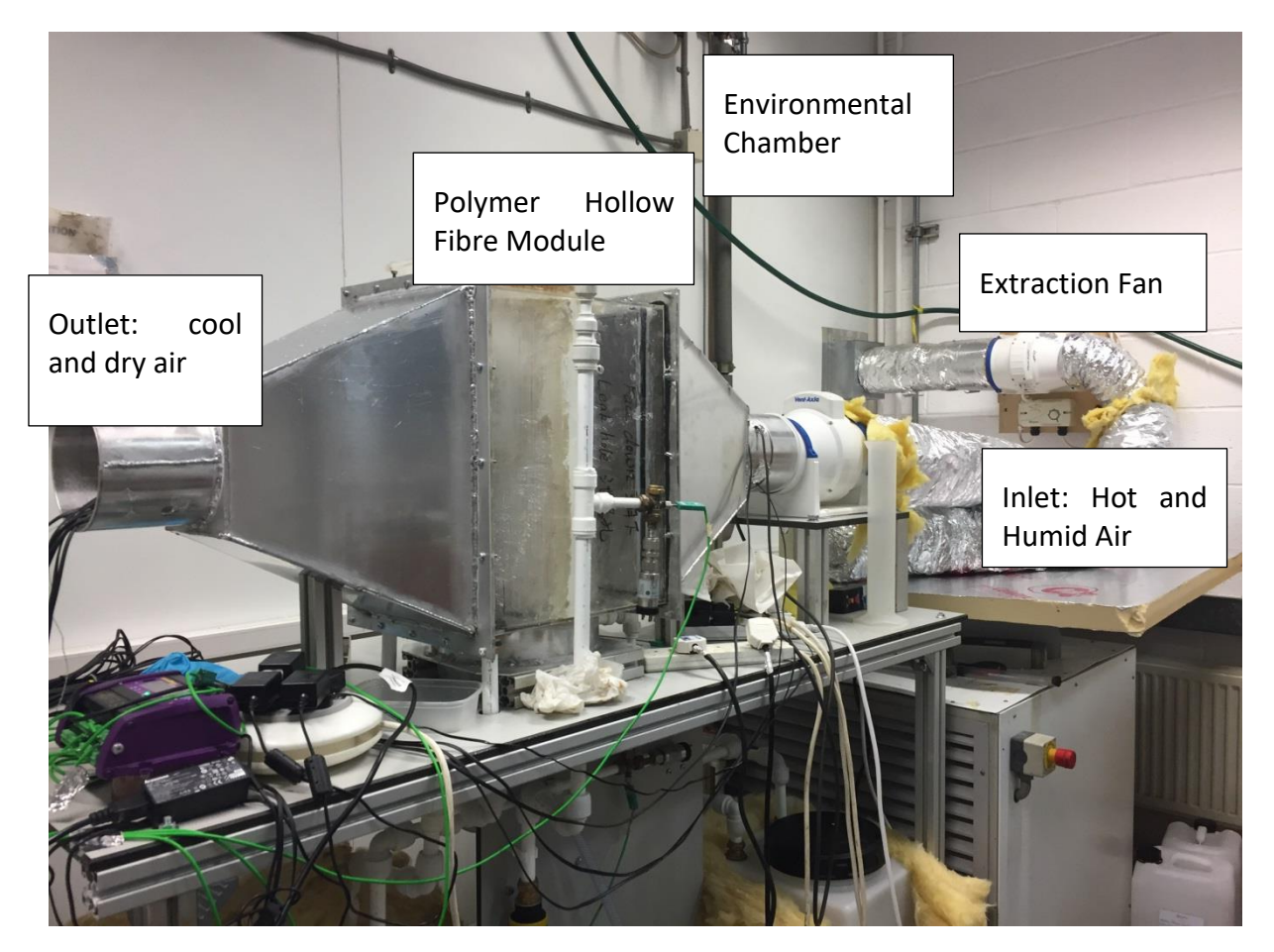


Figure 4(B) the connections with the environmental chamber

Fig. 4.The polymer hollow fibre integrated liquid desiccant dehumidification testing rig (A) and the connections with the environmental chamber (B)

Table 1 Physical properties of the polymer hollow fibre module

Property	Symbol	Values	Unit			
Module cross section diameter	D	0.20	m			
Module height	h	0.5	m			
Fibre number inside the module	N	5000				
Fibre outside diameter	$d_o$	1.6	mm			
Fibre inside diameter	$d_i$	1.4	mm			
Nominal pore size		0.5	μm			
Fibre porosity		0.5				
Packing density		832	m <sup>2</sup> /m <sup>3</sup>			



Packing fraction		0.32	
Polymer hollow fibre thermal conductivity	k	0.17	W/mK
Desiccant solution concentration	X	36%, 49%, 62%	
Incoming air velocity	$\nu_a$	0.65-4.5	m/s
Liquid desiccant flow rate	$m_{sol}$	0.05	I/s
Incoming air temperature	$T_a$	35-40	°C
Incoming air humidity	$\omega_a$	0-75%	



### 3 Design and development of evaporative cooling unit

#### 3.1 Liquid desiccant dehumidification and cooling system

The purpose of the polymer hollow fibre liquid desiccant system is to dehumidify and cool the supplied to building fresh air. The return air (from inside to outside of the building) is used directly in the process of regeneration of the desiccant solution. In Figure 5, the details of the components of the complete system are presented.

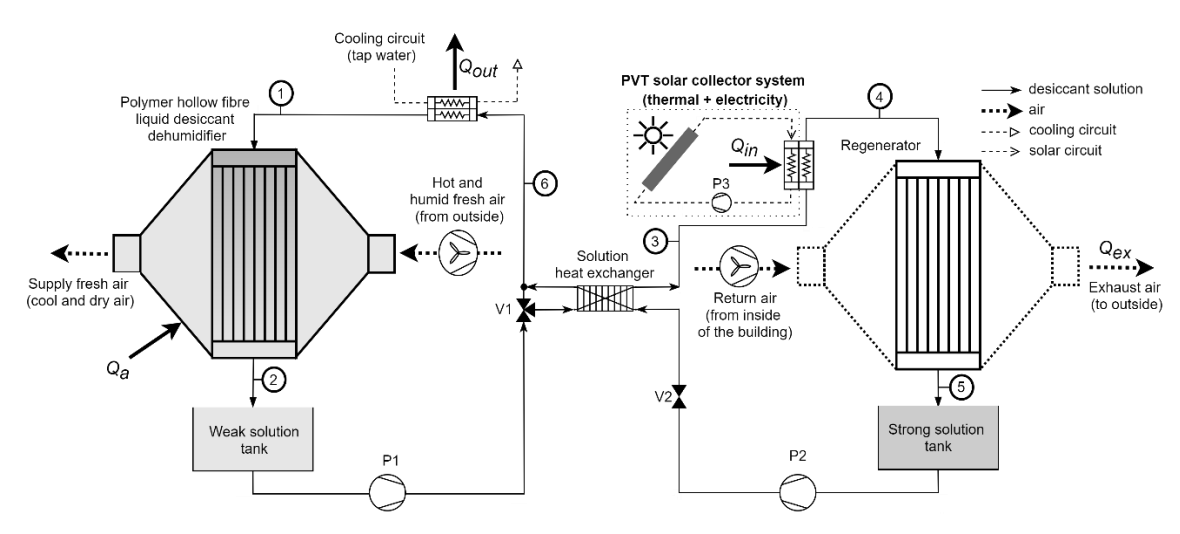


Fig. 5. Polymer hollow fibre liquid desiccant air dehumidification and cooling cycle.

This system consists in two main circuits, which are a cold circuit (on the left of the solution heat exchanger) and hot circuit (on the right of the solution heat exchanger). The cold circuit is where air is dehumidified and cooled, and the hot circuit is the cycle for regeneration of the solution desiccant (remove the excess of water/increase solution concentration). The thermal energy from the PVT solar collector is used to heat the solution and the electricity can be used for the fans and pumps. The complete cycle is divided in six parts, which are:

- Between 1 and 2: Air is dehumidified and cooled, and consequently the concentration of the liquid desiccant solution decreases and the its temperature increase.
- Between 2 and 3: The weak solution is pre-heated by the strong solution.
- Between 3 and 4: The solution is heated up to around 60°C by the PVT solar collector.
- Between 4 and 5: Return air is used to remove the excess of water in the solution in the regenerator. In this process the solution became a strong solution and cooled by the return air.
- Between 5 and 6: The strong solution is pre-cooled by the weak solution.
- Between 6 and 1: The strong solution is cooled by tap water, and the cycle is repeated.

The solution can also be transferred directly from point 2 to 6 if the concentration is higher than an established value. This control is done by valve V1.

#### 3.2 Building and climate description

Regarding integration of the desiccant system in the building, in Figure 6 is presented the configuration proposed in this project. The system is a compact unit, which include all the circuit



and separately we have the two-solution tanks. This configuration has the advantage that it is near the PVT solar collector system, which avoids extra hydraulic circuit for the solar system.

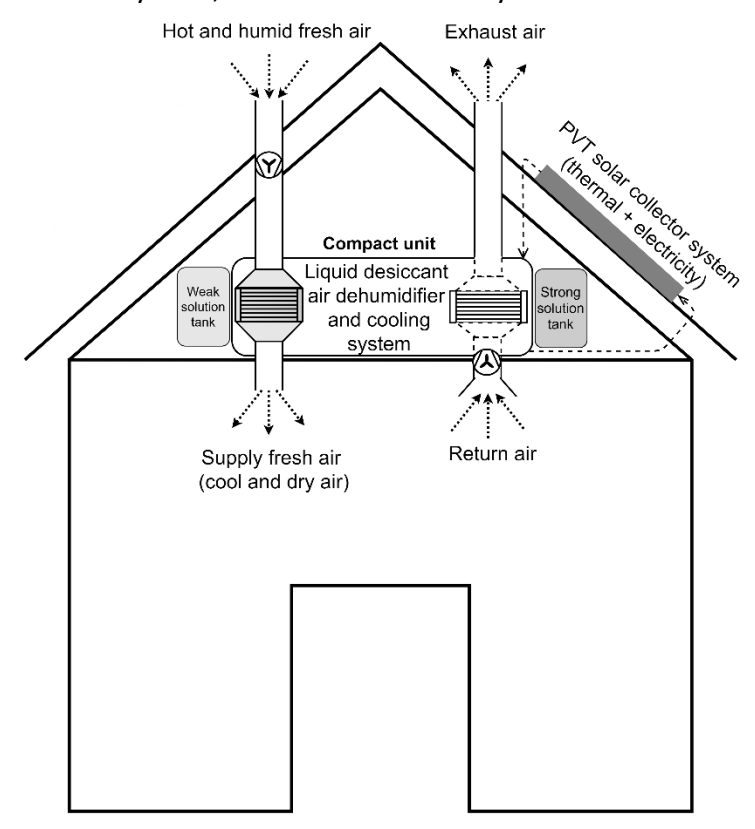


Fig. 6. Diagram of a domestic installation of Liquid desiccant dehumidification and cooling system.

27/04/2022



# 4. System performances

#### 4.1 Effect of the inlet air conditions

The performance of the system is found through calculation of the sensible effectiveness and latent effectiveness, respectively, using:

$$arepsilon_{sen} = rac{ar{T}_{a,out} - T_{a,in}}{T_{s,in} - T_{a,in}}$$
 Eq. (1)

$$arepsilon_{lat} = rac{ar{\omega}_{a,out} - \omega_{a,in}}{\omega_{s,in} - \omega_{a,in}}$$
 Eq. (2)

in which  $T_{a,in}$  and  $T_{s,in}$  are the inlet temperature of air and solution, respectively,  $\bar{T}_{a,out}$  is the mean outlet temperature of air,  $\omega_{a,in}$  and  $\omega_{s,in}$  are the inlet humidity ratio of air and solution, respectively, and  $\overline{\omega}_{a.out}$  is the meat outlet specific humidity of air.

Effectiveness-NTU method has been adopted to analyse the performance of the heat exchangers in terms of non-dimensional variables, as calculated in Eq. (3) - Eq. (4).

$$NTU = \frac{UA_{tot}}{(mC_p)_{min}}$$
 Eq. (3)

$$U = \left[\frac{1}{h_{air}} + \frac{\delta}{k_m} + \frac{1}{h_{sol}}\right]^{-1}$$
 Eq. (4)

Where, U represents for the overall heat transfer coefficient (W/m<sup>2</sup>K).  $A_{tot}$  is the total external surface area of the membrane  $(m^2)$ .  $\dot{m}$  is the mass flow rate (kg/s).  $C_p$  is the specific heat capacity under constant pressure (J/(kg  $\cdot$  K)). ( $\dot{m} \cdot C_p$ ) $_{min}$  is the minimum value of heat capacity rate of the air and desiccant solution (W/K).  $h_{air}$  is the convestive heat transfer coefficient of the air  $(W/(m^2 \cdot K))$ .  $h_{sol}$  is the convestive heat transfer coefficient of the desiccant solution  $(W/(m^2\cdot K))$ .  $\delta$  is the membrane thickness (m).  $K_m$  is the thermal conductivity of the membrane  $(W/m \cdot K)$ .

The number of mass transfer unit  $(NTU_m)$  is a significant parameter to evaluate the latent effectiveness of the heat and mass transfer exchanger, as calculated in Eq. (5)-(6).

$$NTU_m = \frac{U_m A_{tot}}{\dot{m}_{min}}$$
 Eq. (5)

$$NTU_m = \frac{U_m A_{tot}}{\dot{m}_{min}}$$
 Eq. (5)
$$U_m = \left[\frac{1}{h_{m,air}} + \frac{\delta}{k_m} + \frac{1}{h_{m,sol}}\right]^{-1}$$
 Eq. (6)

Where,  $U_m$  is the overall mass transfer coefficient (kg/m2s);  $\dot{m}_{min}$  is the minimum mass flow rate of air and dessicant solution (kg/s),  $h_{m,air}$  is the air convective mass transfer coefficient (kg/m2s);  $h_{m,sol}$  is the convective mass transfer coefficient of the desiccant solution (kg/m2s), which could be neglected for the simplicity due to that the mass transfer coefficient of the desiccant solution is much higher than the air.

According to the numerical analysis results, the inlet air conditions (i.e. inlet air velocity  $V_{air,i}$ , and temperature  $T_{air,i}$ ) are crucial parameters of the proposed PHFD. Fig 7-9 show the variations of 4 parameters: sensible effectiveness, latent effectiveness, outlet air temperature and specific humidity difference under various air velocities. As shown in Fig. 7, with increasing air velocity, the latent capacity ratio ( $m_{lat}$ ) and sensible capacity ratio ( $m_{sen}$ ) will increase while the NTU<sub>m</sub> and NTU will decrease. As demonstrated in Fig. 9, a higher inlet air velocity will cause a rise of the outlet air temperature and the specific humidity difference between the inlet and the outlet air. This will result in the increase of the sensible and latent effectiveness, as shown in Fig.9. For

27/04/2022 20



example, at the inlet air relative humidity of 60% and dry bulb temperature of 35°C, when the inlet air velocity increases from 1.5m/s to 4.5m/s, the specific humidity difference between the inlet air and the outlet air are 0.0040kg/kg, 0.0030kg/kg, 0.0022kg/kg, 0.0018kg/kg respectively, while the sensible and latent effectiveness are 0.381, 0.207, 0.08, 0.03 and 0.383, 0.290, 0.206, 0.178. This is because the higher air velocity leads to the reduction of the contact duration between the incoming air and the desiccant solution inside the PHFD. Therefore, this results in less effective heat and mass transfer, which is reflected by a lower sensible and latent effectiveness, as shown in Fig.8.

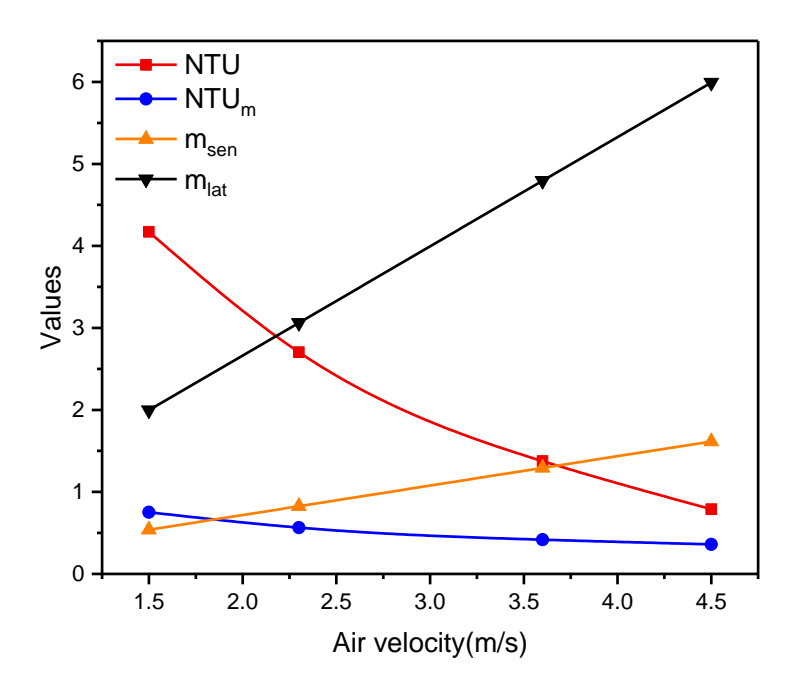
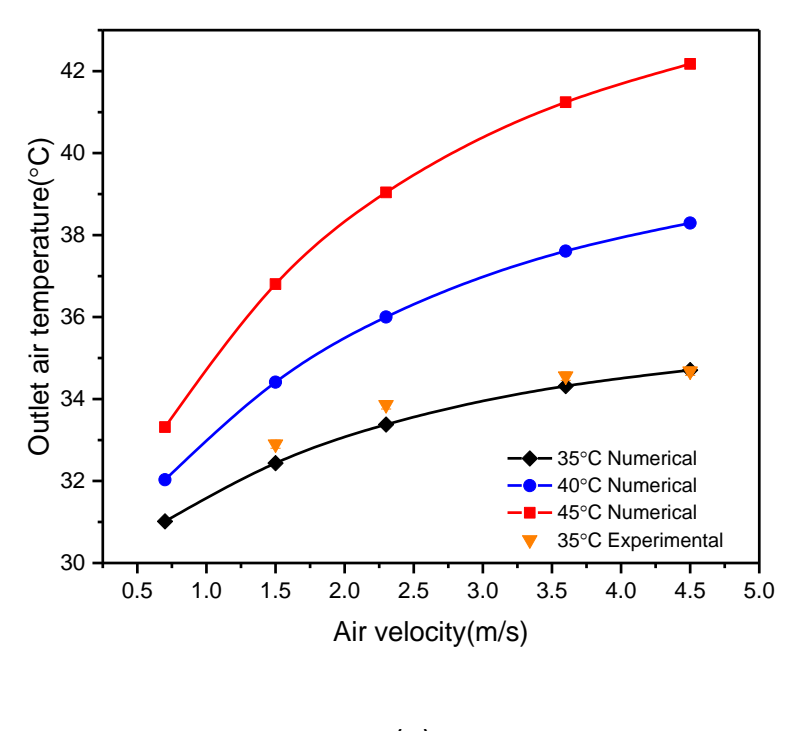


Fig. 7. The dimensionless parameters variations under different air velocities ( $T_{air,i}$ = 35°C,  $T_{sol,i}$ =29.5°C,  $\dot{m}_{sol,i}$ =0.028kg/s, RH<sub>air,i</sub>=60%, X<sub>sol</sub>=62%)







(A)

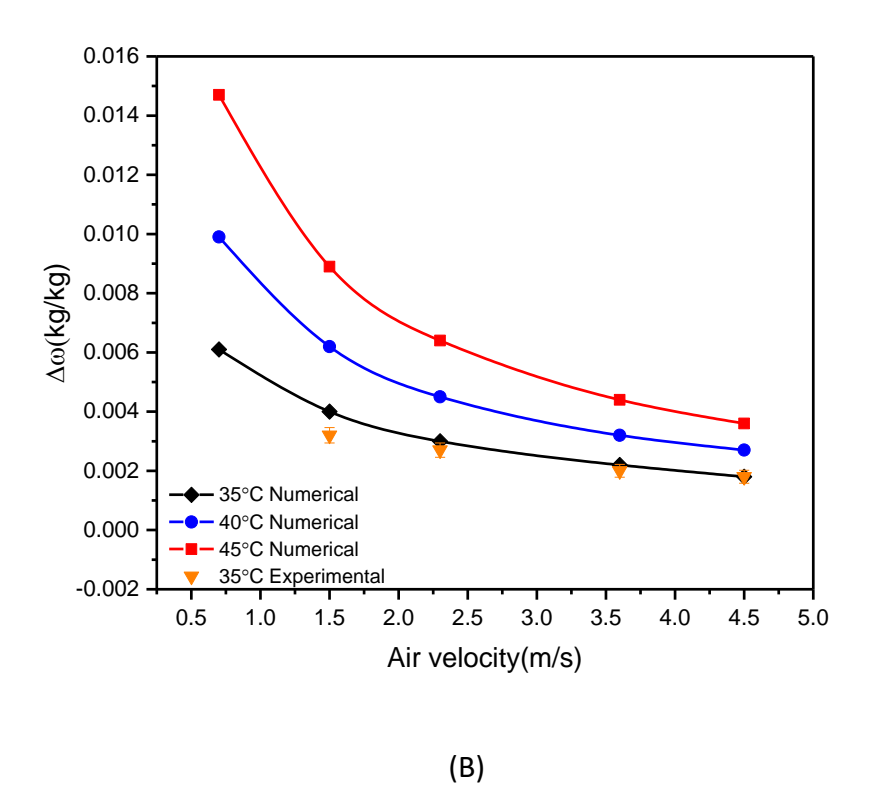
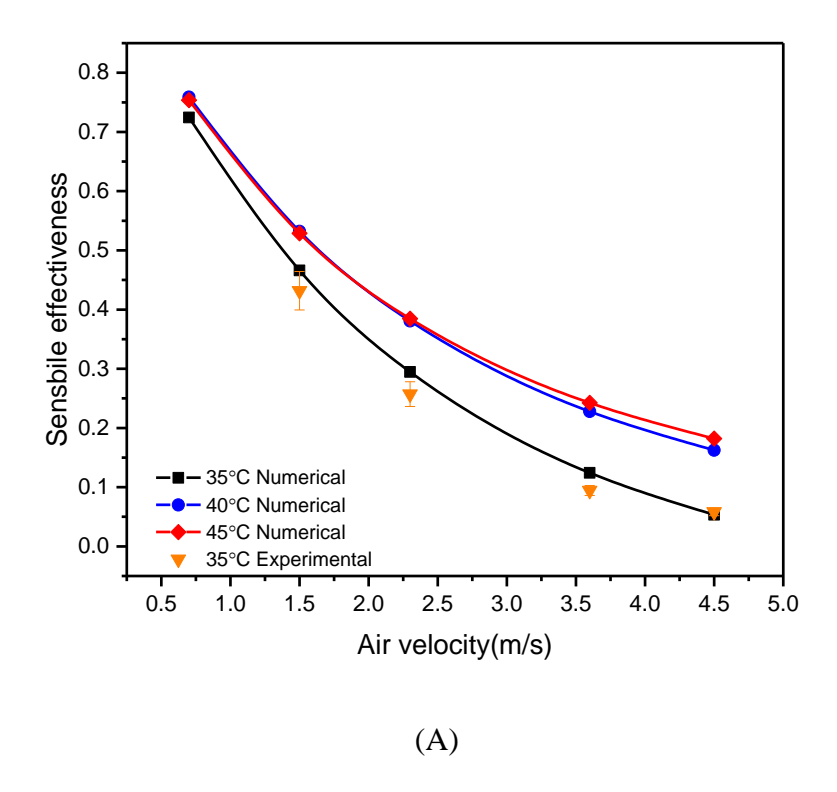


Fig. 8.The numerical obtained outlet air temperature (A) and specific humidity difference (B) under various air velocities ( $T_{sol,i}=29.5^{\circ}C$ ,  $\dot{m}_{sol,i}=0.028$ kg/s, RH<sub>air,i</sub>=60%, X<sub>sol</sub>=62%)





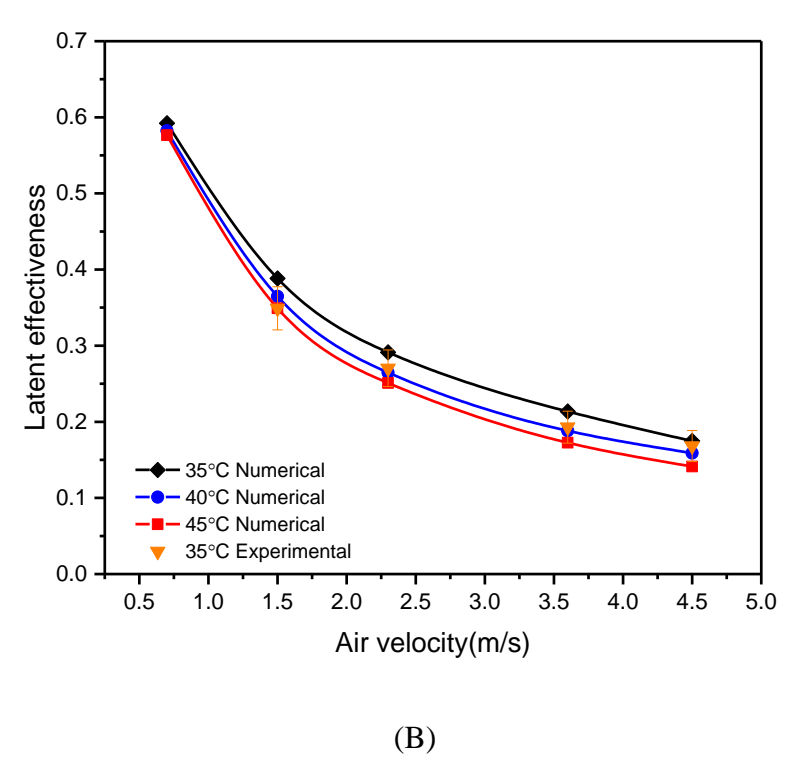


Fig. 9. The numerical obtained sensible effectiveness (A) and latent effectiveness (B) under different inlet air velocities ( $T_{sol,i}$ = 29.5°C,  $\dot{m}_{sol,i}$ =0.028kg/s, RH<sub>air,i</sub>= 60%, X<sub>sol</sub>= 62%)



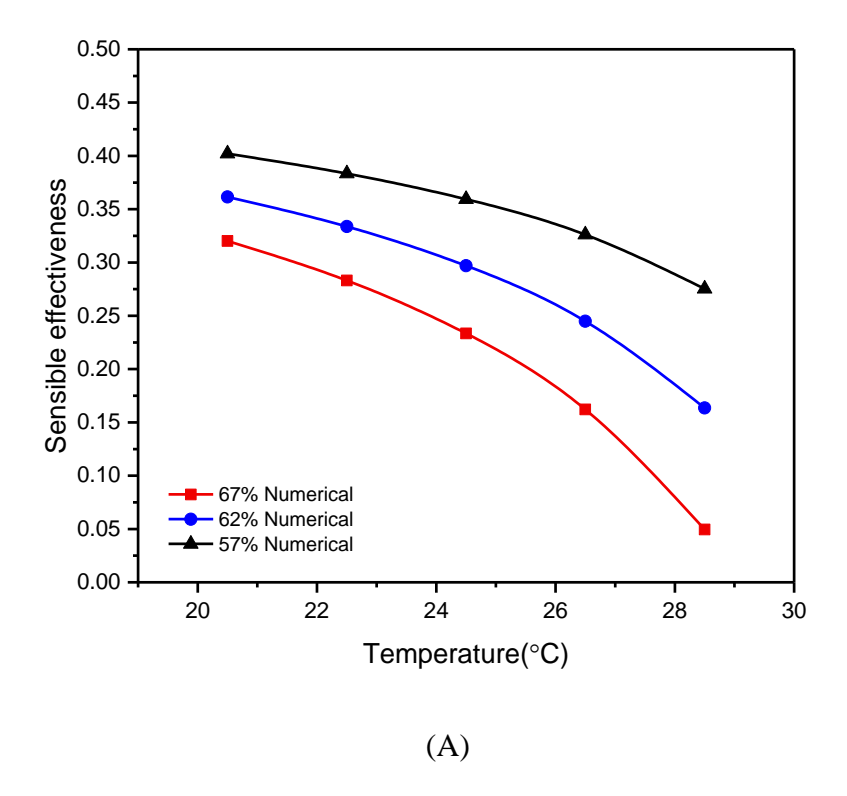
Further reflection on the results shown in Fig. 9(A) reveals that at the fixed solution concentration and inlet air velocity, the sensible effectiveness will increase at a higher air temperature. For instance, when the air velocity is fixed at 3.6m/s, for the inlet air temperature of 35°C, 40°C and 45°C, the sensible effectiveness is 0.12, 0.23 and 0.24, respectively. In contrast, as depicted in Fig. 9 (B), when the solution concentration and the inlet air velocity are fixed, a higher inlet air temperature results in lower latent effectiveness. For instance, the latent effectiveness only decreases by 1.6% and 1% respectively when the inlet air temperature increases from 35°C to 40°C and 40 to 45°C at 0.7m/s air velocity, which is negligible. On the contrary,  $\Delta\omega$  increases with temperature when the velocity of the inlet air is 0.7m/s. The reason of this is that the increase of the inlet air temperature will lead to higher specific humidity, while the inlet equilibrium humidity of the solution remains unchanged and increases the vapor pressure difference indirectly.

#### 4.2 Effect of the liquid desiccant solution inlet conditions

The temperature of the solution and its concentration also play a crucial role in the dehumidification performance. Figure 10 indicates the variations of the sensible and latent effectiveness under several inlet solution temperatures at various concentrations. As it can be found from Fig.10(A), the sensible effectiveness drops with the increase of the solution temperature. For example, at a 57% concentration, the sensible effectiveness varies from 0.4 to 0.3 when the solution temperature changes from 20.5°C to 28.5°C. It should be noted that at higher solution temperatures, high-concentration solutions are more sensitive to temperature changes. For instance, as the temperature of the solution rises from 26.5°C to 28.5°C, the sensible effectiveness at a 57% concentration drops by 15%. In contrast, when the concentration is 62%, the corresponding decrease is 32%. In Fig. 10(B), it can be seen that the latent effectiveness almost remains constant as the solution temperature rises. For instance, at a 62% concentration, the latent effectiveness is 0.203, 0.200, 0.200, 0.200, 0.198 at the solution temperature of 20.5°C, 22.5°C, 24.5°C, 26.5°C, 28.5°C, respectively. This is because, the solution equilibrium humidity (KCOOH) is related to its temperature and concentration. Although the vapor pressure will naturally increase with the solution temperature, the solution equilibrium humidity will also increase, and will thus reduce both the nominator and denominator. In addition, lower solution concentration leads to lower latent effectiveness, for example, at 26.5°C, the latent effectiveness is 0.22, 0.20, and 0.18 for the concentration ratios of 67%, 62%, 57%, respectively.







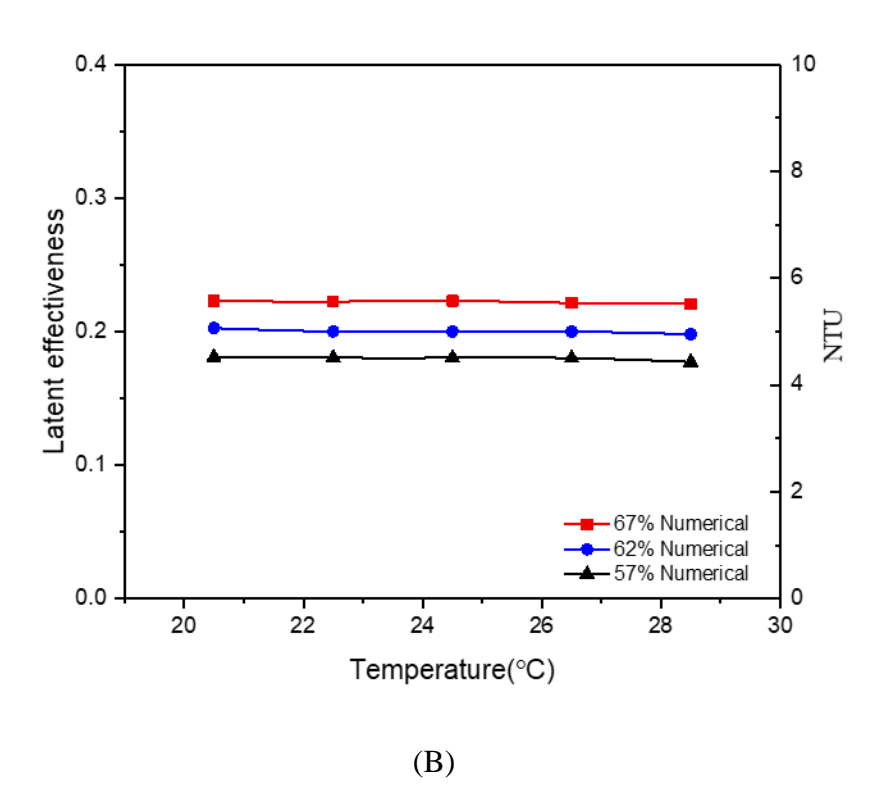


Fig. 10. Variations of sensible effectiveness (A) and latent effectiveness (B) for several inlet solution temperatures at various solution concentrations ( $T_{air,i}=35^{\circ}C$ ,  $RH_{air,i}=60\%$ ,  $V_{air,i}=3.6$ m/s,  $\dot{m}_{sol,i}=0.028$ kg/s)



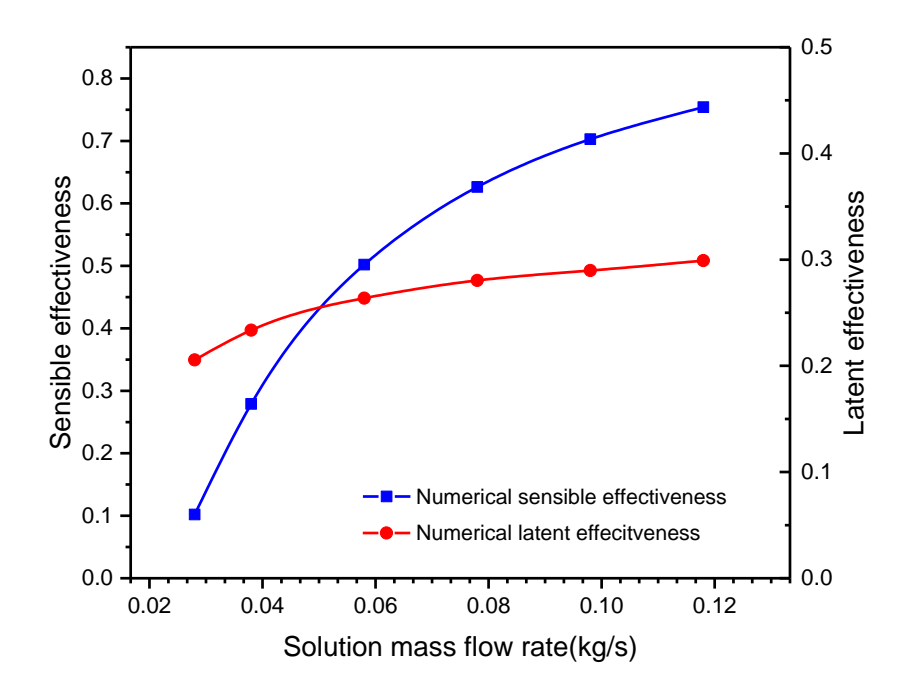


Fig. 11. Variations of latent and sensible effectiveness with the solution mass flow rate (Tair,i= 35°C, Tsol,i= 29.5°C, RHair,i= 60%, Xsol= 62%, Vair,i= 3.6m/s)

#### 4.3 Effects of the dimensionless parameters

The influences of the air to solution specific humidity ratio  $\omega_r^*$  on the outlet air temperature, the sensible effectiveness, the specific humidity difference, the moisture removal rate, the latent effectiveness, and the total effectiveness are demonstrated in Figs. 12-14. The other initial air and solution conditions were invariable, the air velocity at the inlet were fixed at 0.7m/s, the inlet air temperature was fixed at 35 °C, and the inlet solution mass flow rate was 0.028 kg/s. As shown in Fig. 12, the air temperature at the outlet rises from 30.6 °C to 31.8 °C (an increase of 3.9%) and the sensible effectiveness drops from 0.79 to 0.57 (a fall of 22%) when the  $\omega_r^*$  varies between 1.46 and 2.12. Inspection of Fig. 13 indicates that the air specific humidity difference and the moisture removal rate both increase when the  $\omega_r^*$  increases. For instance, the air specific humidity difference is 0.0053 kg/kg, 0.0065 kg/kg, 0.0079 kg/kg, 0.0089 kg/kg, 0.0098 kg/kg and 0.0106 kg/kg at  $\omega_r^*$  of 1.46, 1.62, 1.78, 1.88, 1.99 and 2.12, respectively, and the rate of moisture removal raised by 104% (from 0.21kg/s to 0.43kg/s) at each  $\omega_r^*$ . The reason is that higher  $\omega_r^*$ indicates a higher water vapor pressure. No matter whether the inlet air specific humidity increases, or the inlet solution concentration decreases, a greater vapor pressure difference between incoming air and desiccant solution is reached. This leads to the solution attracting more moisture from the inlet air, which increases the specific humidity difference between the inlet air and the outlet air. When the desiccant solution absorbs more vapor, a higher amount of latent heat will be released. This results in a smaller temperature difference between the incoming air and the desiccant solution, which makes the temperature drop gradually.



As shown in Fig. 14, the impact of the air to solution specific humidity ratio on the latent effectiveness is negligible. For example, the latent effectiveness is kept around 0.61, when  $\omega_r^*$  changes from 1.45 to 2.15. On the other hand, the total effectiveness decreases with the increase of  $\omega_r^*$ . This is because although the air-specific humidity or solution equilibrium humidity increase dramatically with the rise of  $\omega_r^*$ , the air specific humidity difference between the air and the solution at the inlet also grows. Thus, the latent and total effectiveness are not affected by  $\omega_r^*$ .

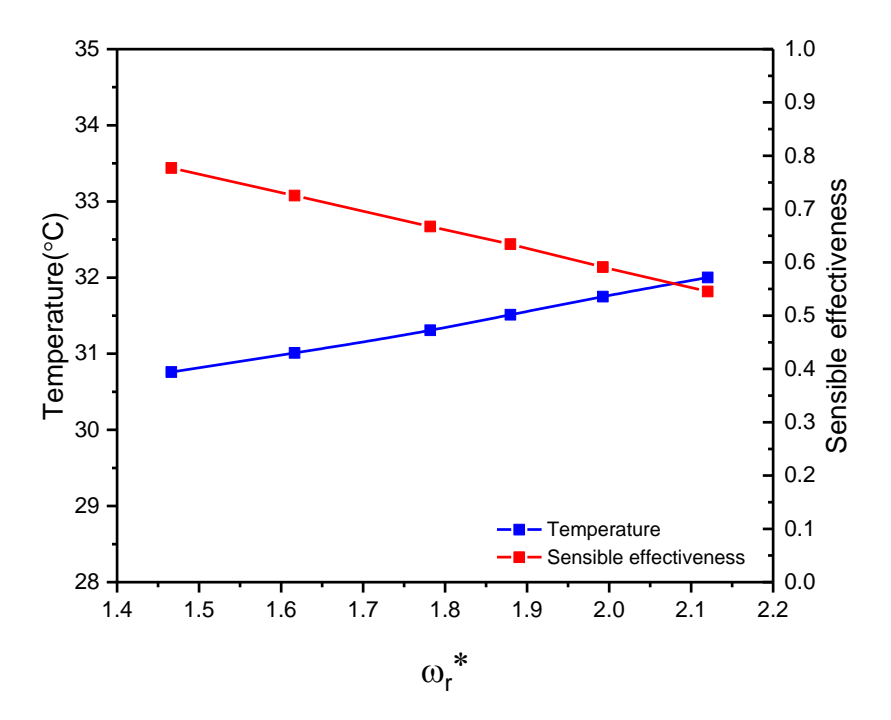


Fig. 12. Variation of the outlet air temperature and sensible effectiveness with the air to solution specific humidity ratio ( $T_{air,i}=35^{\circ}C$ ,  $T_{sol,i}=29.5^{\circ}C$ ,  $\dot{m}_{sol,i}=0.028$ kg/s,  $V_{air,i}=3.6$ m/s)



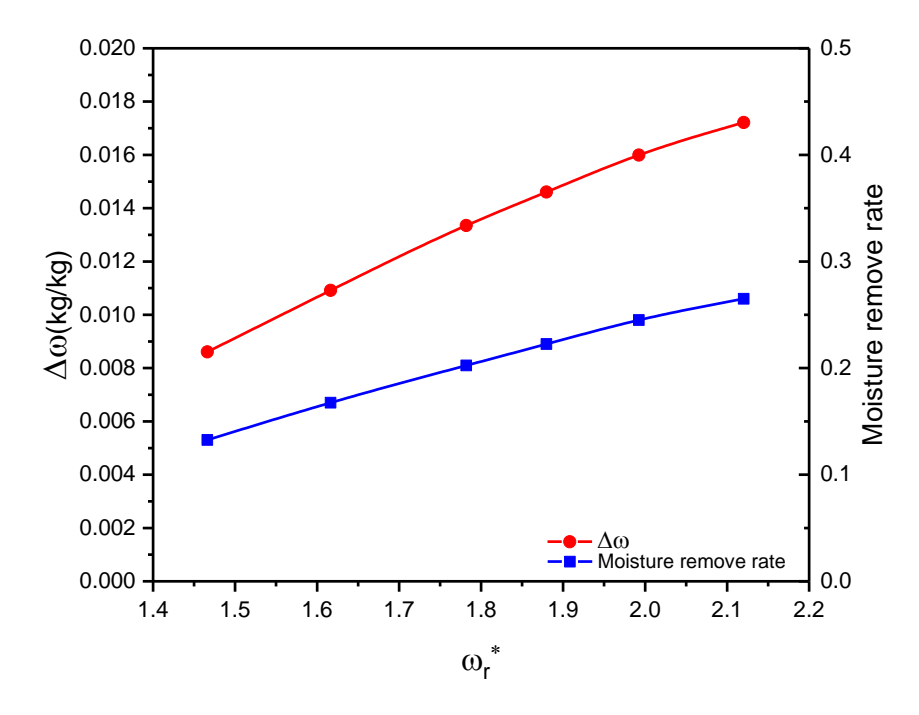


Fig. 13. Variation of the specific humidity difference and moisture removal rate with the air to solution specific humidity ratio ( $T_{air,i}=35^{\circ}C$ ,  $T_{sol,i}=29.5^{\circ}C$ ,  $\dot{m}_{sol,i}=0.028$ kg/s,  $V_{air,i}=3.6$ m/s)

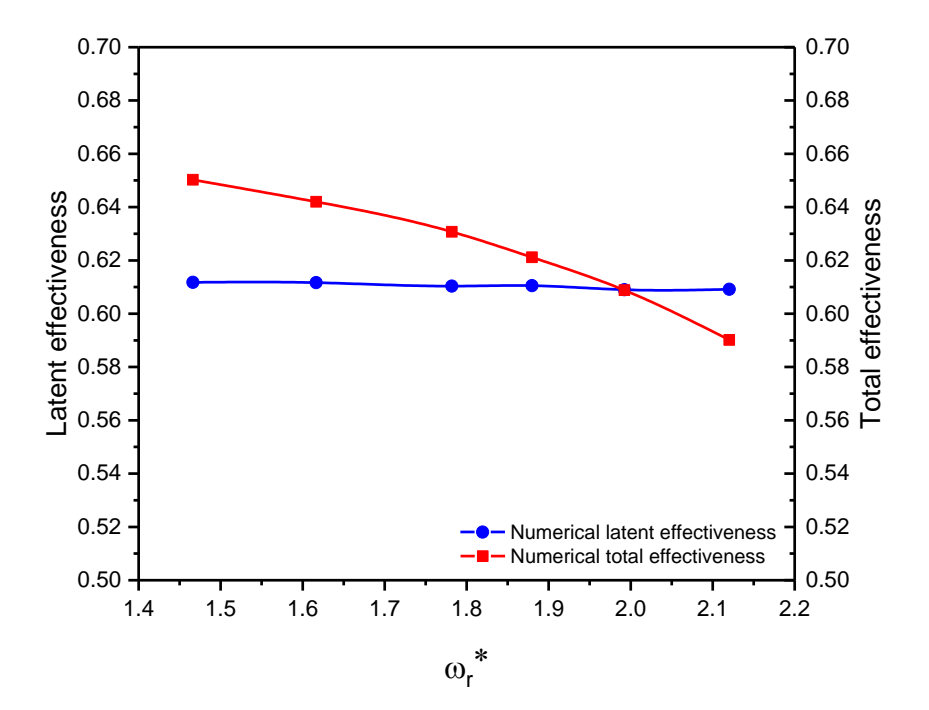


Fig. 14. Variation of the latent effectiveness and total effectiveness with the air to solution specific humidity ratio  $(T_{air,i}=35 \, ^{\circ}\text{C} , T_{sol,i}=29.5 \, ^{\circ}\text{C} , \dot{m}_{sol,i}=0.028 \, \text{kg/s}, V_{air,i}=3.6 \, \text{m/s})$ 

To summarise, the variation of air velocity has strong effect on  $T_{ao}$ ,  $\omega_{ao}$ , NTU, NTU<sub>m</sub>,  $m_{sen}$ ,  $m_{lat}$ , and has a significant effect on the latent effectiveness and the sensible effectiveness. The



sensible effectiveness and total effectiveness are less related to  $\omega_r^*$ . The moisture removal rate and the sensible effectiveness change significantly with the variations of  $\omega_r^*$ . Meanwhile, the change of air specific humidity difference and the inlet and outlet air temperature difference are closely related to  $\omega_r^*$ . It implies that changes of the  $\omega_r^*$  within a certain range (i.e. 1.45 to 2.15) is preferable for increasing the dehumidification performance without reducing the latent effectiveness.



#### **Conclusions**

In this work package, the development and construction of evaporative cooling unit has been completed. Its accuracy has been validated and its no-load operation has been checked. Optimisation and functional tests with materials are necessary as part of work package 4 previously to the demo site works phase. In this deliverable, the design of this evaporative cooling unit has been detailed. The different components of the system have been explained, regarding hardware (electric, control, mechanical, safety and external systems, room controller and central controller). Finally, the construction of the prototype for the SUREFIT Project has been documented. It is important to note that although these developments are considered of great interest in different types of environment, the normative regarding these kind of systems is not ready yet, so it is not clear whether it will finally be possible their installation in any of the demo sites planned in the project. Anyway, this technology will be validated at laboratory scale and the possibility of use in a demo site is being studied.



## References

- 1. Choudhury, B., P.K. Chatterjee, and J.P. Sarkar, Review paper on solar-powered air-conditioning through adsorption route. Renewable and Sustainable Energy Reviews, 2010. 14(8): p. 2189-2195.
- 2. Adnott, J., Energy Efficiency of Room Air-conditioners (EERAC) Study, Directorate General for Energy (DGXVII) of the Commission of the European Communities. 1999.
- 3. Chen, X., et al., Theoretical studies of a hybrid ejector CO2 compression cooling system for vehicles and preliminary experimental investigations of an ejector cycle. Applied Energy, 2013. 102: p. 931-942.
- 4. Chen, X., et al., Recent developments in ejector refrigeration technologies. Renewable and Sustainable Energy Reviews, 2013. 19: p. 629-651.
- 5. Wang, R.Z. and R.G. Oliveira, Adsorption refrigeration—An efficient way to make good use of waste heat and solar energy. Progress in Energy and Combustion Science, 2006. 32(4): p. 424-458.
- 6. Duan, Z., et al., Indirect evaporative cooling: Past, present and future potentials. Renewable and Sustainable Energy Reviews, 2012. 16(9): p. 6823-6850.
- 7. Farmahini-Farahani, M., S. Delfani, and J. Esmaeelian, Exergy analysis of evaporative cooling to select the optimum system in diverse climates. Energy, 2012. 40(1): p. 250-257.
- 8. Liao, C.-M. and K.-H. Chiu, Wind tunnel modeling the system performance of alternative evaporative cooling pads in Taiwan region. Building and Environment, 2002. 37(2): p. 177-187.
- 9. Rawangkul, R., et al., Performance analysis of a new sustainable evaporative cooling pad made from coconut coir. International Journal of Sustainable Engineering, 2008. 1(2): p. 117-131.
- 10. He, S., et al., Experimental study of film media used for evaporative pre-cooling of air. Energy Conversion and Management, 2014. 87: p. 874-884.
- 11. Mujahid Rafique, M., et al., A review on desiccant based evaporative cooling systems. Renewable and Sustainable Energy Reviews, 2015. 45: p. 145-159.
- 12. Alahmer, A., Thermal analysis of a direct evaporative cooling system enhancement with desiccant dehumidification for vehicular air conditioning. Applied Thermal Engineering, 2016. 98: p. 1273-1285.
- 13. Riangvilaikul, B. and S. Kumar, An experimental study of a novel dew point evaporative cooling system. Energy and Buildings, 2010. 42(5): p. 637-644.
- 14. Caliskan, H., et al., Thermodynamic performance assessment of a novel air cooling cycle: Maisotsenko cycle. International Journal of Refrigeration, 2011. 34(4): p. 980-990.
- 15. Zhao, X., J.M. Li, and S.B. Riffat, Numerical study of a novel counter-flow heat and mass exchanger for dew point evaporative cooling. Applied Thermal Engineering, 2008. 28(14–15): p. 1942-1951.



- 16. Zhao, X., et al., Feasibility study of a novel dew point air conditioning system for China building application. Building and Environment, 2009. 44(9): p. 1990-1999.
- 17. Wu, J.M., X. Huang, and H. Zhang, Numerical investigation on the heat and mass transfer in a direct evaporative cooler. Applied Thermal Engineering, 2009. 29(1): p. 195-201.
- 18. Franco, A., et al., Influence of water and air flow on the performance of cellulose evaporative cooling pads used in mediterranean greenhouses. Transactions of the ASABE, 2010. 53(2): p. 565-576.
- 19. Johnson, D.W., C. Yavuzturk, and J. Pruis, Analysis of heat and mass transfer phenomena in hollow fiber membranes used for evaporative cooling. Journal of Membrane Science, 2003. 227(1–2): p. 159-171.
- 20. Chen, X., et al., Recent research developments in polymer heat exchangers A review. Renewable and Sustainable Energy Reviews, 2016. 60: p. 1367-1386.
- 21. Chiari, A., Air humidification with membrane contactors: experimental and theoretical results. International journal of ambient energy, 2000. 21(4): p. 187-195.
- 22. Wickramasinghe, S.R., M.J. Semmens, and E.L. Cussler, Hollow fiber modules made with hollow fiber fabric. Journal of Membrane Science, 1993. 84(1): p. 1-14.
- 23. Chen, X., et al., Experimental investigations of polymer hollow fibre heat exchangers for building heat recovery application. Energy and Buildings, 2016. 125: p. 99-108.
- 24. Kachhwaha, S.S. and S. Prabhakar, Heat and mass transfer study in a direct evaporative cooler. Journal of Scientific & Industrial Research, 2010. 69: p. 705-710.
- 25. Daou, K., R.Z. Wang, and Z.Z. Xia, Desiccant cooling air conditioning: a review. Renewable and Sustainable Energy Reviews, 2006. 10(2): p. 55-77.
- 26. La, D., et al., Technical development of rotary desiccant dehumidification and air conditioning: A review. Renewable and Sustainable Energy Reviews, 2010. 14(1): p. 130-147.
- 27. Longo, G.A. and A. Gasparella, Experimental and theoretical analysis of heat and mass transfer in a packed column dehumidifier/regenerator with liquid desiccant. International Journal of Heat and Mass Transfer, 2005. 48(25–26): p. 5240-5254.
- 28. Fumo, N. and D.Y. Goswami, Study of an aqueous lithium chloride desiccant system: air dehumidification and desiccant regeneration. Solar Energy, 2002. 72(4): p. 351-361.
- 29. Dai, Y.J. and H.F. Zhang, Numerical simulation and theoretical analysis of heat and mass transfer in a cross flow liquid desiccant air dehumidifier packed with honeycomb paper. Energy Conversion and Management, 2004. 45(9–10): p. 1343-1356.
- 30. Liu, J., et al., Experimental analysis of an internally-cooled/heated liquid desiccant dehumidifier/regenerator made of thermally conductive plastic. Energy and Buildings, 2015. 99: p. 75-86.
- 31. Lazzarin, R.M., A. Gasparella, and G.A. Longo, Chemical dehumidification by liquid desiccants: theory and experiment. International Journal of Refrigeration, 1999. 22(4): p. 334-347.



- 32. Koronaki, I.P., et al., Thermodynamic analysis of a counter flow adiabatic dehumidifier with different liquid desiccant materials. Applied Thermal Engineering, 2013. 50(1): p. 361-373.
- 33. Longo, G.A. and A. Gasparella, Three years experimental comparative analysis of a desiccant based air conditioning system for a flower greenhouse: Assessment of different desiccants. Applied Thermal Engineering, 2015. 78: p. 584-590.
- 34. Riffat, S.B., S.E. James, and C.W. Wong, Experimental analysis of the absorption and desorption rates of HCOOK/H2O and LiBr/H2O. International Journal of Energy Research, 1998. 22(12): p. 1099-1103.